第 32 卷第 3 期
2016 年 3 月

无 机 化 学 学 报
CHINESE JOURNAL OF INORGANIC CHEMISTRY

Vol.32 No.3
499-507

Li_3PO_4 表面修饰提高球形 $LiNi_{0.5}Mn_{1.5}O_4$ 正极材料的性能

任 宁* 卢世刚*
(北京有色金属研究总院,北京 100088)

摘要: 通过共沉淀法制备了球形 $LiNi_{0.5}Mn_{1.5}O_4$@Li_3PO_4 复合材料,并采用 X 射线衍射(XRD)、扫描电镜(SEM)、红外光谱(FT-IR)、循环伏安 (CV)、电化学阻抗谱 (EIS) 及充放电测试研究了其结构与电化学性能。XRD 和 SEM 表明,Li_3PO_4 包覆影响了球形 $LiNi_{0.5}Mn_{1.5}O_4$ 的晶格常数。CV 和 EIS 表明,质量百分数 5% Li_3PO_4 包覆的 $LiNi_{0.5}Mn_{1.5}O_4$ 具有比纯 $LiNi_{0.5}Mn_{1.5}O_4$ 更高的锂离子嵌脱可逆性,更大的锂离子扩散系数和更小的电荷转移电阻,说明在锂离子扩散过程中,质量百分数 5%Li_3PO_4 包覆的 $LiNi_{0.5}Mn_{1.5}O_4$ 具有更高的电子电导率。充放电测试表明,原位 Li_3PO_4 改性提高了材料的电子电导率、电化学活性,进而提高了高倍率放电容量。质量百分数 5% Li_3PO_4 包覆的 $LiNi_{0.5}Mn_{1.5}O_4$ 提高的电化学性能归因于 Li_3PO_4 的包覆、纳米颗粒组成球形的粒径引起的高的电子电导率和小的电化学极化。

关键词: 锂离子电池; 正极材料; 表面包覆; 电化学性能
中图分类号: O646.21; TM912.9 **文献标识码**: A **文章编号**: 1001-4861(2016)03-0499-09
DOI: 10.11862/CJIC.2016.068

Li_3PO_4 Surface Modification to Improve Performance of $LiNi_{0.5}Mn_{1.5}O_4$ Cathode Material

REN Ning* LU Shi-Gang*
(*General Research Institute for Nonferrous Metals, Beijing* 100088, *China*)

Abstract: Spherical $LiNi_{0.5}Mn_{1.5}O_4$@Li_3PO_4 composite was prepared by a co-precipitation method. The structure and electrochemical performance were investigated by X-ray powder diffraction (XRD), scanning electron microscope (SEM), FT-IR spectroscopy, cyclic voltammetry (CV), electrochemical impedance spectroscopy (EIS) and charge-discharge measurements. XRD and SEM shows that Li_3PO_4 coating influence the lattice parameter of $LiNi_{0.5}Mn_{1.5}O_4$ composed of spherical particle size. CV and EIS imply that 5% (mass percent) Li_3PO_4-coated $LiNi_{0.5}Mn_{1.5}O_4$ has higher reversible intercalation and deintercalation of Li^+, larger lithium-ion diffusion coefficient and smaller charge transfer resistance corresponding to a much higher conductivity than those of pristine $LiNi_{0.5}Mn_{1.5}O_4$ corresponding to the extraction of Li^+ ions. Charge-discharge test reveals that the *in situ* Li_3PO_4 modifying improves the electronic conductivity of the electrode in the local environment, electrochemical activity, and then results in their relatively higher capacity at high charge-discharge rate. The enhanced performance of 5% (mass percent) Li_3PO_4-coated $LiNi_{0.5}Mn_{1.5}O_4$ is ascribed to the improved electronic conduction and the reduced polarization resulting from the Li_3PO_4 modification together with sphere-like particles composed of nano particle $LiNi_{0.5}Mn_{1.5}O_4$.

Keywords: lithium-ion battery; cathode materials; surface coating; electrochemical performance

收稿日期:2015-08-31。收修改稿日期:2015-11-26。
*通信联系人。E-mail:rnrm040412@163.com,lusg8867@163.com

0 Introduction

Spinel $LiMn_2O_4$ is one of the most promising cathode for electric vehicles (EVs), hybrid electrical vehicles (HEVs), and plug-in hybrid vehicles (PHEVs) due to its adequate capacity, economical production, safety, low toxicity and high thermal stability [1]. Unfortunately, poor rate capability, cyclability and high-temperature performance limit its further application for power batteries due to the Jahn-Teller distortion[2]. In addition, a further improvement in terms of cycling life and energy density is still required to fulfill the demands of these applications. As we know, the partial substitution by other metals for Mn in $LiMn_2O_4$ could stabilize the crystal structure and improve the cycling performance[3-5]. Among all doped $LiM_xMn_{2-x}O_4$, the Ni-doped spinel $LiNi_{0.5}Mn_{1.5}O_4$ has attracted great interests for its good rate capability, high theoretical capacity (147 $mAh \cdot g^{-1}$) and much high discharge voltage at around 4.7 V corresponding to the redox reactions of Ni^{2+}/Ni^{3+} and Ni^{3+}/Ni^{4+} redox couples[6]. However, $LiNi_{0.5}Mn_{1.5}O_4$ usually losses oxygen and disproportionates to a spinel and $Li_xNi_{1-x}O$ or NiO when it is heated above 650 ℃ [7]. Hence, this $LiNi_{0.5}Mn_{1.5}O_4$ compound still has a non-negligible capacity fading during cycling due to the structural and chemical instabilities resulted from the presence of high spin Mn^{3+} ions. Hence, morphology controlling[8], doping[9-12] and surface coating[13-17] were considered as effective ways to improve the electrochemical performance of $LiNi_{0.5}Mn_{1.5}O_4$ materials. Various morphologies of $LiNi_{0.5}Mn_{1.5}O_4$, such as nanoparticles[18], nanorods[19], and microspheres[20], have been successfully fabricated to improve the electrochemical performance. However, nanomaterial frequently results in a low volumetric energy density of the cell. A variety of methods used to prepare $LiNi_{0.5}Mn_{1.5}O_4$ have been developed, including solid-state reaction[21], sol-gel[22], emulsion drying[23], composite carbonate process[24], hydrothermal method[25] and co-precipitation[26]. Among those routes to preparation of cathode materials, the co-precipitation is one of the most effective and conventional and inexpensive methods to synthesize the final product of $LiNi_{0.5}Mn_{1.5}O_4$[27]. Li_3PO_4 is known to be a fast solid lithium ionic conductor[28], and Li_3PO_4 coating has been used to improve the electrochemical performance of $LiMn_2O_4$[29], $LiCoO_2$[30], $LiFePO_4$[31] cathode materials. With this consideration, we have developed a novel ethanol-assisted co-precipitation method to synthesize spherical $LiNi_{0.5}Mn_{1.5}O_4$ and Li_3PO_4-coated $LiNi_{0.5}Mn_{1.5}O_4$ composites. With this method, the Mn^{3+} in the $LiNi_{0.5}Mn_{1.5}O_4$ can be efficiently limited. Consequently, the overall electrochemical performance of the $LiNi_{0.5}Mn_{1.5}O_4$ can be obviously improved.

1 Experimental

1.1 Material preparation

For the preparation of Li_3PO_4, a certain amount of LiOH and H_3PO_4 was dissolved in deionized water, and then heated in water bath with mechanical stirring at 80 ℃ for 6 h. Then the turbid liquid was filtered, and dried in vacuum drying oven for 12 h at 120 ℃, yielding Li_3PO_4 powders. $LiNi_{0.5}Mn_{1.5}O_4$ powders were prepared by ethanol-assisted oxalic acid co-precipitation method. The $NiSO_4 \cdot 6H_2O$ and $MnSO_4 \cdot H_2O$ were dissolved in the mixed solution of deionized water and ethanol with a molar ratios of 1∶2, and named solution 1. The NH_4HCO_3 was also dissolved in the deionized water, and the molar ratio between NH_4HCO_3 and sulphate ($NiSO_4 \cdot 6H_2O$+$MnSO_4 \cdot H_2O$) is 1∶1, and named solution 2. The solution 1 and solution 2 were mixed, and then the resulting precursor solution was transferred to a Teflon-lined stainless steel autoclave and heated at 200 ℃ for 10 h. The powder deposited at the bottom of the reactor was collected by centrifugation. The powder and appropriate Li_2CO_3 was mixed, then the precursors were heat treated at 800 ℃ for 12 h at ambient condition, and then treated at 600 ℃ for 6 h, and then air-cooled to the room temperature, yielding $LiNi_{0.5}Mn_{1.5}O_4$ dark powders.

For the preparation of $LiNi_{0.5}Mn_{1.5}O_4$@Li_3PO_4, the Li_3PO_4 was added to the mixture of solution 1 and solution 2, and transferred to a Teflon-lined stainless steel autoclave and heated at 200 ℃ for 10 h. The following synthesis process is the same for

$LiNi_{0.5}Mn_{1.5}O_4$ powders. The predetermined amounts of Li_3PO_4 in $LiNi_{0.5}Mn_{1.5}O_4$ are 5% and 10% (mass percent), respectively.

1.2 Material characterization

The crystal structure was characterized by X-ray diffractometry (XRD) measurements performed on a Rigaku instrument with Cu $K\alpha_1$ radiation (45 kV, 50 mA, step size=0.02°, 10°<2θ<90°). The morphology and the microstructure of the products were examined by a scanning electron microscopy (SEM, SU8000). FT-IR spectroscopy of the samples was performed using a Nicolet Nexus 6700 FT-IR spectrophotometer with a resolution of 4 cm^{-1}. A total of 1.5 mg sample dried at 120 ℃ was thoroughly mixed with 200 mg KBr and pressed into pellets and the scans were performed immediately to avoid water absorption. The frequency range was 800~400 cm^{-1}.

1.3 Electrochemical analysis

The electrochemical characterizations were performed using CR2025 coin-type cell. The working electrode was prepared by mixing 80% (mass percent) active material, 10% (mass percent) conductive super P carbon and 10% (mass percent) polyvinylidene fluoride (PVDF) as binder in N-methyl pyrrolidinone (NMP). After being uniformly coated onto a copper foil, the slurry was dried in a vacuum at 120 ℃ for 10 h. A solution of 1 mol·L^{-1} $LiPF_6$ dissolved in a mixture of ethylene carbonate and dimethyl carbonate (1:1, in volume) was used as the electrolyte and porous polypropylene Celgard 2300 was used as separator. The charge-discharge measurements were recorded on multichannel Land Battery Test System (Wuhan Jinnuo, China) at room temperature between 3.5 and 4.95 V (vs Li/Li^+) carried out at different charge-discharge rates. Cyclic voltammetry (CV) test was carried out on a CHI 1000C electrochemical workstation with a voltage between 3.5 and 4.95 V at a scanning rate of 0.05 mV·s^{-1}. Electrochemical impedance spectroscopy (EIS) of OCV (open circuit voltage, before cycle) is measured by a Princeton P4000 electrochemical working station over a frequency range from 0.01 Hz to 10 kHz at a potentiostatic signal amplitude of 5 mV. The open circuit voltage is about 3.2 V.

2 Results and discussion

Fig.1 shows the X-ray diffraction patterns of the pristine and Li_3PO_4 coated-$LiNi_{0.5}Mn_{1.5}O_4$ powders. All the sharp diffraction peaks can be attributed to the well-defined cubic spinel structure of $LiNi_{0.5}Mn_{1.5}O_4$. This indicates that the Li_3PO_4 coating does not change the spinel structure of $LiNi_{0.5}Mn_{1.5}O_4$. In addition, no trace of impurity phase (such as $Li_xNi_{1-x}O$ or NiO) is detected. However, the characteristic Li_3PO_4 diffraction peak is not obvious, indicating that the Li_3PO_4 in the $LiNi_{0.5}Mn_{1.5}O_4/Li_3PO_4$ composites are amorphous during the calcination process. The strong reflections located at 19.1°, 36.8°, 38.5°, 44.5°, 48.8°, 58.9°, 64.8°, 68.1°, 76.6° and 77.6° can be indexed to the (111), (311), (222), (400), (331), (511), (440), (531), (533) and (620) diffractions, respectively. It is well known that $LiNi_{0.5}Mn_{1.5}O_4$ has two different space groups, $Fd\bar{3}m$ or $P4_332$ depending on Ni ordering in the lattice. In the $Fd\bar{3}m$ structure, Li^+ ions occupy the tetrahedral (8a) sites; Mn or Ni ions reside at the octahedral (16d) sites random; and O^{2-} ions are located at (32e) sites. In $P4_332$ structure the Li atoms are located at 8c sites, Ni atoms at 4a sites, Mn atoms at 12d sites, and O atoms at 8c and 24e sites[32-33]. In $LiNi_{0.5}Mn_{1.5}O_4$ with $P4_332$ space group, it can be found a decrease of lattice parameter and symmetry caused by cation ordering, and weak superstructure reflections

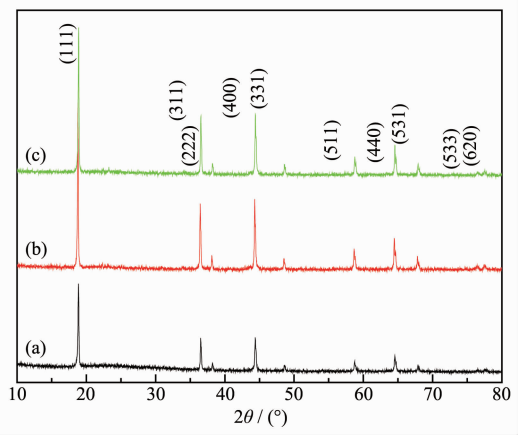

Fig.1 XRD pattern of pristine and coated $LiNi_{0.5}Mn_{1.5}O_4$ (a) pristine $LiNi_{0.5}Mn_{1.5}O_4$; (b) 5% Li_3PO_4 coated-$LiNi_{0.5}Mn_{1.5}O_4$; (c) 10% Li_3PO_4 coated-$LiNi_{0.5}Mn_{1.5}O_4$

around $2\theta \approx 15°$, 24°, 35°, 40°, 46°, 47°, 57°, and 75° can be found [34]. However, the scanning rate in this work was too fast for us to detect them.

In fact, the structural difference between these two space groups is hardly to be clearly distinguished by X-ray diffraction because of the similar scattering factors of Ni and Mn. FT-IR spectroscopy has proved to be an effective technique in qualitatively resolving the cation ordering (Fig.2). It has been reported that the peak at about 623 cm^{-1} in $Fd\bar{3}m$ phase are more intensive than those at 593 cm^{-1}, which is contrary to the $P4_332$ phase[35]. In addition, three new peaks at about 650, 470 and 432 cm^{-1} are absent in $Fd\bar{3}m$ structure. Hence, it can be concluded that pristine $LiNi_{0.5}Mn_{1.5}O_4$ and 10% Li_3PO_4-coated $LiNi_{0.5}Mn_{1.5}O_4$ has a space $P4_332$ groups. However, the peak of 5% Li_3PO_4-coated $LiNi_{0.5}Mn_{1.5}O_4$ at about 623 cm^{-1} are weaker than that at 593 cm^{-1}, revealing that 5% Li_3PO_4-coated $LiNi_{0.5}Mn_{1.5}O_4$ has a $P4_332$ and $Fd\bar{3}m$ mixed phase. This indicates that 5% Li_3PO_4-coated $LiNi_{0.5}Mn_{1.5}O_4$ has the biggest degree of disorder among all samples. It has been reported that the crystal with disordered space groups have the better transmission path of electronic and Li^+ [36]. Therefore, it can be concluded that the 5% Li_3PO_4-coated $LiNi_{0.5}Mn_{1.5}O_4$ has the better electrochemical performance than ordered $LiMn_{1.5}Ni_{0.5}O_4$ and 10% Li_3PO_4-coated $LiNi_{0.5}Mn_{1.5}O_4$.

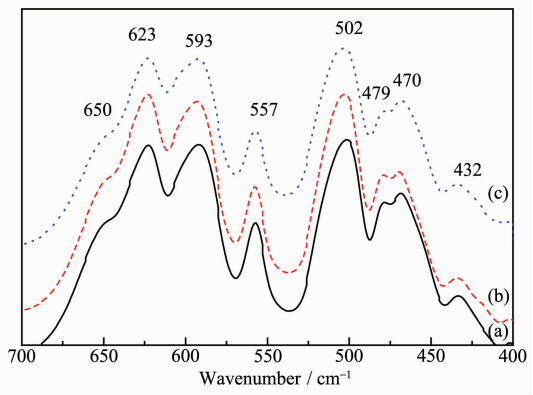

Fig.2 FT-IR of pristine and coated $LiNi_{0.5}Mn_{1.5}O_4$ (a) pristine $LiNi_{0.5}Mn_{1.5}O_4$; (b) 5% Li_3PO_4 coated-$LiNi_{0.5}Mn_{1.5}O_4$; (c) 10% Li_3PO_4 coated-$LiNi_{0.5}Mn_{1.5}O_4$

Fig.3 shows the SEM images of the pristine and Li_3PO_4 coated-$LiNi_{0.5}Mn_{1.5}O_4$ powders. It can be found that the particles of all samples exist as homogeneous sphere-like particles. The diameters of the spheres distribute within the range of 1~1.5 μm. The sphere-like particles are composed of nano particle $LiNi_{0.5}Mn_{1.5}O_4$ at about 100 nm. Very small particles of coated $LiNi_{0.5}Mn_{1.5}O_4$ powders were found to be highly dispersed on the coated Li_3PO_4 particles as shown in Fig.3b and Fig.3c. In addition, the surface morphology of pristine $LiNi_{0.5}Mn_{1.5}O_4$ is extremely smooth. From a comparison of this three powders surface morphology, it can be speculated that the surface of the prepared $LiNi_{0.5}Mn_{1.5}O_4$ is covered with small Li_3PO_4. This indicates that the surface modification leads to formation of uniform coating.

Fig.4 examines the initial charge and discharge behaviors of a series of Li_3PO_4-coated $LiNi_{0.5}Mn_{1.5}O_4$ materials at room temperature in 3.5~4.95 V range, at a current density of 0.2C. The initial discharge capacities of pristine and 5, 10% Li_3PO_4-coated $LiNi_{0.5}Mn_{1.5}O_4$ cathode material are 118.1, 131.6 and 132.9 $mAh \cdot g^{-1}$, respectively. Obviously, Li_3PO_4 coating increases the initial discharge capacity of $LiNi_{0.5}Mn_{1.5}O_4$ cathode.

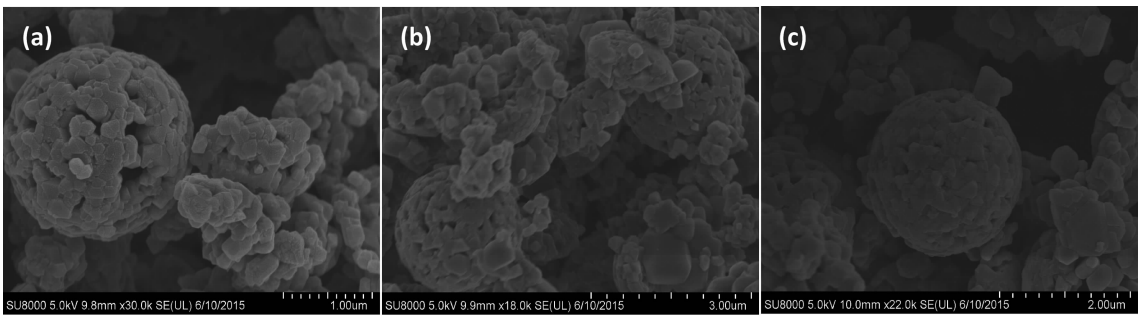

Fig.3 SEM images of pristine and coated $LiNi_{0.5}Mn_{1.5}O_4$ (a) pristine $LiNi_{0.5}Mn_{1.5}O_4$; (b) 5% Li_3PO_4 coated-$LiNi_{0.5}Mn_{1.5}O_4$; (c) 10% Li_3PO_4 coated-$LiNi_{0.5}Mn_{1.5}O_4$

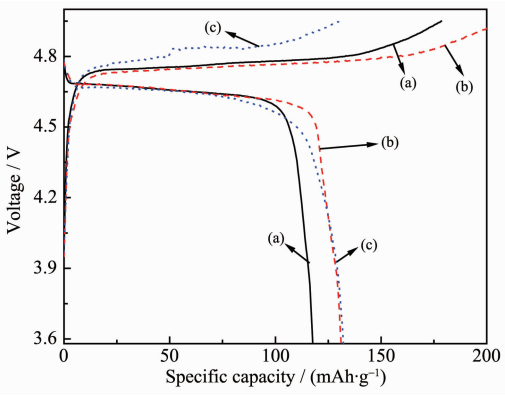

Fig.4　Initial charge-discharge curves of pristine and coated $LiNi_{0.5}Mn_{1.5}O_4$ (a) pristine $LiNi_{0.5}Mn_{1.5}O_4$; (b) 5% Li_3PO_4 coated-$LiNi_{0.5}Mn_{1.5}O_4$; (c) 10% Li_3PO_4 coated-$LiNi_{0.5}Mn_{1.5}O_4$

Fig.5 shows the rate capabilities for three samples. The cells were discharged at increasingly higher currents from 0.2C to 0.5C rates at room temperature. It can be found that the capacity difference between the pristine $LiNi_{0.5}Mn_{1.5}O_4$ electrode and 5% Li_3PO_4-coated $LiNi_{0.5}Mn_{1.5}O_4$ electrode progressively increased. At the 0.5C charge-discharge rate after 20 cycles, the discharge capacity was 107.4 $mAh\cdot g^{-1}$ for the pristine $LiNi_{0.5}Mn_{1.5}O_4$ material (90.9% of the capacity at 0.2C), and 120 $mAh\cdot g^{-1}$ for the 5% Li_3PO_4-coated $LiNi_{0.5}Mn_{1.5}O_4$ material (91.2% at 0.2C). This result indicates that the Li_3PO_4 coating improves the rate capability of $LiNi_{0.5}Mn_{1.5}O_4$ as well as its capability to store Li ions. The reason may be suggested as follows.

Trace water impurity in the electrolyte would

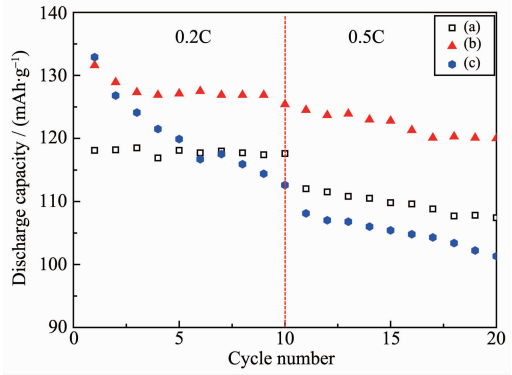

Fig.5　Rate performance of pristine and coated $LiNi_{0.5}Mn_{1.5}O_4$ (a) pristine $LiNi_{0.5}Mn_{1.5}O_4$; (b) 5% Li_3PO_4 coated-$LiNi_{0.5}Mn_{1.5}O_4$; (c) 10% Li_3PO_4 coated-$LiNi_{0.5}Mn_{1.5}O_4$

cause the liberation of acid HF through the decomposition of $LiPF_6$-based electrolyte. The chemical reactions were proposed as follows[37-38]:

$$LiF_6+H_2O\rightarrow LiF+2HF+POF_3 \quad (1)$$

$$POF_3+H_2O\rightarrow PO_2F_2^-+HF \quad (2)$$

HF will dissolve $LiNi_{0.5}Mn_{1.5}O_4$ proposed as follows[39]:

$$4HF+2LiNi_{0.5}Mn_{1.5}O_4\rightarrow 3Ni_{0.25}Mn_{0.75}O_2+0.25NiF_2+0.75MnF_2+2LiF+2H_2O \quad (3)$$

Therefore, it can be concluded that a uniform Li_3PO_4 coating on the surface of the $LiNi_{0.5}Mn_{1.5}O_4$ not only can act as an ion-conductive layer, but also acts to suppress the decomposition of Mn and Ni during cycling, as demonstrated in Fig.6. However, 10% Li_3PO_4-coated $LiNi_{0.5}Mn_{1.5}O_4$ electrode shows an unsatisfactory rate performance, indicating that the contents of coated Li_3PO_4 have strong impact on the rate capability of $LiNi_{0.5}Mn_{1.5}O_4$ electrode. Therefore, it is important to optimize the coated Li_3PO_4 content in order achieve a good cell performance.

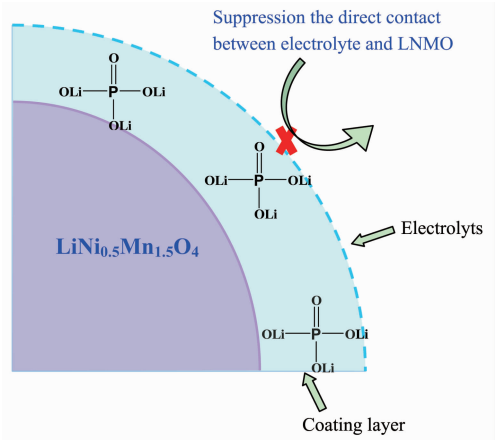

Fig.6　Schematic illustration of how the Li_3PO_4 layer acts as a conductive and protective layer to suppress the direct contact between electrolyte and LNMO and decomposition of electrolyte

Fig.7 presents typical cyclic voltammograms (CVs) of pristine and Li_3PO_4 coated-$LiNi_{0.5}Mn_{1.5}O_4$. The intense and sharp reduction/oxidation peaks of Ni^{2+}/Ni^{4+} are observed at around 4.7 V in pristine and Li_3PO_4 coated-$LiNi_{0.5}Mn_{1.5}O_4$, with trace amount of the couple of Mn^{4+}/Mn^{3+} that usually appears at around 4.0 V shown in inset. The appearance of 4 V peak was due to Mn^{3+} which was formed by the oxygen loss

during high temperature calcinations. It can be found that the CV curve of pristine $LiNi_{0.5}Mn_{1.5}O_4$ presents a much more obvious redox peaks in the potential region around 4.0 V (from the redox couples Mn^{4+}/Mn^{3+}), which means that the oxygen deficiency is more severe from the oxygen loss due to the Li_3PO_4 coating[40]. This indicates that Li_3PO_4 coating destroys the ordering of Ni and Mn ions, and the proportion of $Fd\bar{3}m$ spinel increase with the rise of Li_3PO_4 content.

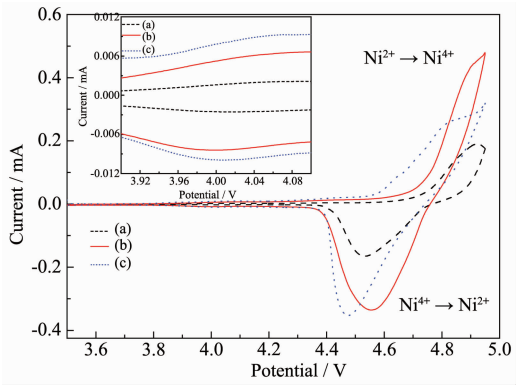

Fig.7 CV curves of pristine and coated $LiNi_{0.5}Mn_{1.5}O_4$ (a) pristine $LiNi_{0.5}Mn_{1.5}O_4$; (b) 5% Li_3PO_4 coated-$LiNi_{0.5}Mn_{1.5}O_4$; (c) 10% Li_3PO_4 coated-$LiNi_{0.5}Mn_{1.5}O_4$

The potential differences between anodic and cathodic peaks reflect the polarization degree of the electrode[41]. The potential difference of the pristine and Li_3PO_4 coated-$LiNi_{0.5}Mn_{1.5}O_4$ electrodes between oxidation and reduction peaks is listed in Table 1. It can be found that the potential difference ($\Delta\varphi_p=\varphi_{pa}-\varphi_{pc}$) of pristine $LiNi_{0.5}Mn_{1.5}O_4$ is 393 mV, obviously much larger than those for the pristine and Li_3PO_4 coated-$LiNi_{0.5}Mn_{1.5}O_4$ electrodes. 5% Li_3PO_4-coated $LiNi_{0.5}Mn_{1.5}O_4$ sample shows the lowest potential interval between anodic and cathodic peak (353 mV), which indicate that the right amount of Li_3PO_4 coating is favorable for reducing the electrode polarization. This means that 5% Li_3PO_4 coated-$LiNi_{0.5}Mn_{1.5}O_4$ has the excellent electrochemical reversibility and faster lithium insertion/extraction kinetics. This observation confirms that right amount of Li_3PO_4 coating enhances the reversibility of the $LiNi_{0.5}Mn_{1.5}O_4$, and then exhibits reversibility and good rate capability.

The kinetics of lithium ion extraction and insertion of the pristine and Li_3PO_4 coated-$LiNi_{0.5}Mn_{1.5}O_4$ electrodes were further investigated by EIS. Fig.8 shows the Nyquist plots of all samples, and the inset is the equivalent circuit used to fit impedance spectra. The circuit consists of R_s (ohmic resistance), R_f (the resistance of a solid electrolyte interphase film), C_f (the capacitance of a solid electrolyte interphase film), R_{ct} (charge-transfer resistance), C_{dl} (double layer capacitance for lithium-ion intercalation) and W (Warburg impedance of solid phase diffusion)[42-43]. The fitted results are summarized in Table 2.

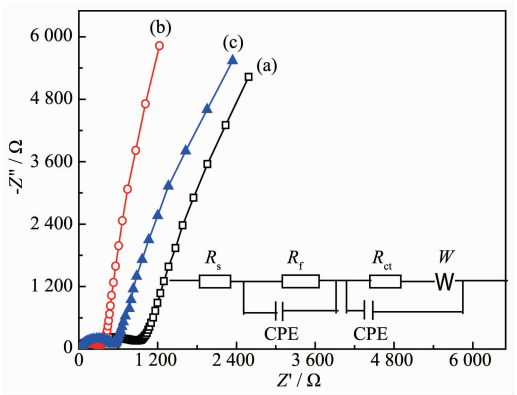

Fig.8 Nyquist plots of pristine and coated $LiNi_{0.5}Mn_{1.5}O_4$ (a) pristine $LiNi_{0.5}Mn_{1.5}O_4$; (b) 5% Li_3PO_4 coated-$LiNi_{0.5}Mn_{1.5}O_4$; (c) 10% Li_3PO_4 coated-$LiNi_{0.5}Mn_{1.5}O_4$

The R_s reflects electric conductivity of the electrolyte, separator, and electrodes. It can be found that 5% Li_3PO_4 coated-$LiNi_{0.5}Mn_{1.5}O_4$ has the smallest ohmic resistance among all samples, indicating a high conductivity between electrolyte and electrodes. Table 2 shows that the charge transfer resistance of Li_3PO_4 coated-$LiNi_{0.5}Mn_{1.5}O_4$ electrode is much lower than that of the pristine one. This reveals that Li_3PO_4 modification is favorable to improve upon the electronic cond-

Table 1 Peak potential differences of CV test for pristine and coated $LiNi_{0.5}Mn_{1.5}O_4$ material

Sample	φ_{pa} / V	φ_{pc} / V	$\Delta\varphi_p$ / mV
$LiNi_{0.5}Mn_{1.5}O_4$	4.924	4.531	393
5% Li_3PO_4-coated $LiNi_{0.5}Mn_{1.5}O_4$	4.920	4.567	353
10% Li_3PO_4-coated $LiNi_{0.5}Mn_{1.5}O_4$	4.855	4.473	382

Table 2　Some fitting parameters obtained by EIS

Sample	R_s / Ω	R_{ct} / Ω	i_0 / (mA·cm^{-2})	D_{Li} / (cm^2·s^{-1})
$LiNi_{0.5}Mn_{1.5}O_4$	9.488	1 855	0.009	7.89×10^{-17}
5% Li_3PO_4-coated $LiNi_{0.5}Mn_{1.5}O_4$	6.684	545	0.031	2.72×10^{-16}
10% Li_3PO_4-coated $LiNi_{0.5}Mn_{1.5}O_4$	7.158	802	0.021	6.11×10^{-17}

uctivity. In addition, 5% Li_3PO_4 coated-$LiNi_{0.5}Mn_{1.5}O_4$ has the smallest charge transfer resistance among all samples. It is reasonable to infer that the lowest charge transfer resistance of 5% Li_3PO_4 coated-$LiNi_{0.5}Mn_{1.5}O_4$ electrode corresponds with the smallest electrochemical polarization, and then lead to the best electrochemical performance. Afterwards, the exchange current density, i_0, can be calculated by means of the charge transfer resistance,

$$i_0=\frac{RT}{AR_{ct}F} \tag{4}$$

where R is the gas constant (8.314 5 J·mol^{-1}·K^{-1}); T is the absolute temperature (298.15 K); F is the Faraday′s constant (96 485 C·mol^{-1}), and A is the area of the electrode surface (1.54 cm^2). The calculated results are given in Table 2. Obviously, 5% Li_3PO_4 coated-$LiNi_{0.5}Mn_{1.5}O_4$ has the biggest c exchange current density among all samples, revealing the lowest intercalation/deintercalation resistance and highest electrochemical activity.

As we know, lithium ion diffusion rate also plays an important role in accelerating lithium ion insertion/extraction during the charge/discharge process[44]. The diffusion coefficient of lithium ion (D_{Li}) can be calculated from the plots in the low frequency region, and can be obtained according to the following equations[45]:

$$Z_{re}=R_{ct}+R_s+\sigma\omega^{-1/2} \tag{5}$$

$$D_{Li}=\frac{R^2T^2}{2A^2n^4F^4C_{Li}^4\sigma^2} \tag{6}$$

where ω is the angular frequency in the low frequency region; R is the gas constant (8.314 5 J·mol^{-1}·K^{-1}); T is the absolute temperature (298.15 K); n is the number of electrons transferred in the half-reaction for the redox couple (n=1); F is the Faraday′s constant (96 485 C·mol^{-1}); A is the area of the electrode surface (1.54 cm^2); C_{Li} is the molar concentration of Li^+ ions calculated by the molar volume (2.37×10^{-2} mol·cm^{-3})[46], and σ is the Warburg impedance coefficient, which is relative to Z_{re}-σ can be obtained from the slope of the lines in Fig.9.

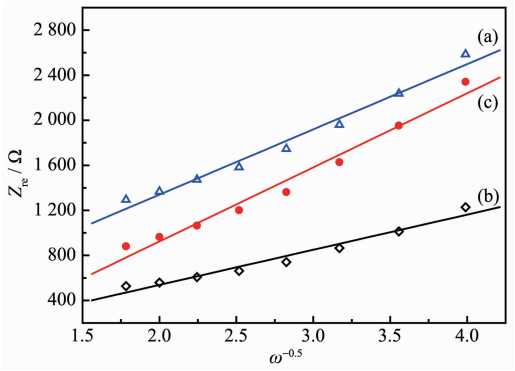

Fig.9　Graph of Z_{re} plotted against $\omega^{-1/2}$ in the low-frequency region for the pristine and coated $LiNi_{0.5}Mn_{1.5}O_4$ (a) pristine $LiNi_{0.5}Mn_{1.5}O_4$; (b) 5% Li_3PO_4 coated-$LiNi_{0.5}Mn_{1.5}O_4$; (c) 10% Li_3PO_4 coated-$LiNi_{0.5}Mn_{1.5}O_4$

The calculated diffusion coefficient of lithium ion is given in Table 2. For the 5% Li_3PO_4-coated $LiNi_{0.5}Mn_{1.5}O_4$, lithium-ion diffusion coefficient is estimated to be 2.72×10^{-16} cm^2·s^{-1}, which is larger than that of 7.89×10^{-17} cm^2·s^{-1} for pristine $LiNi_{0.5}Mn_{1.5}O_4$ cathode. Considering the similar particle sizes and morphologies of three samples, it can be concluded that the improved lithium-diffusivity might be attributed to the modification of Li_3PO_4. Based on the above calculation, the charge transfer resistance and lithium-ion diffusion coefficient indicate that Li_3PO_4 coating can enhance the conductivity of $LiNi_{0.5}Mn_{1.5}O_4$, enabling much easier charge transfer at the interface between the electrode and the electrolyte.

Beaulieu et al reported that lithium ions can react with the grain boundary phase in polycrystalline materials or the liquid electrolyte at the solid/liquid interface[47]. According to the model of the $LiNi_{0.5}Mn_{1.5}O_4$-Li_3PO_4 composites shown in Fig.10, *in situ* coated

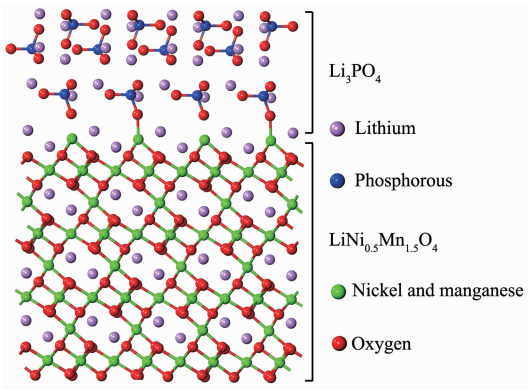

Fig.10 Model of the $LiNi_{0.5}Mn_{1.5}O_4$-Li_3PO_4 composites

Li_3PO_4 is tightly combined with $LiNi_{0.5}Mn_{1.5}O_4$, and then many $LiNi_{0.5}Mn_{1.5}O_4$-Li_3PO_4 phase interfaces can be formed. Li_3PO_4 is a super ionic conductors, and the Li ionic conductivity of Li_3PO_4 (about 10^{-6} $S \cdot m^{-1}$) facilitates the charge transfer reactions on the electrode/electrolyte interface[48]. The combination of in situ coated Li_3PO_4 can improve the Li diffusion coefficient and reduce the charge transfer resistance. The $LiNi_{0.5}Mn_{1.5}O_4$-Li_3PO_4 phase interfaces can also store electrolyte and provide more places for the insertion/extraction reactions of lithium ions, and then improve the reaction kinetics and reduce electrochemical polarization during cycling. Thus it may be a reason for the superior high rate capability of Li_3PO_4-coated $LiNi_{0.5}Mn_{1.5}O_4$. Hence, Li_3PO_4 in situ modification is an effective way to improve the electrochemical performance of $LiNi_{0.5}Mn_{1.5}O_4$.

3 Conclusions

Surface modification of the spherical $LiNi_{0.5}Mn_{1.5}O_4$ is successfully done by Li_3PO_4 coating by the precipitation method. The combination of *in situ* coated Li_3PO_4 can improve the Li diffusion coefficient and reduce the charge transfer resistance of $LiNi_{0.5}Mn_{1.5}O_4$, and then provides more places for the insertion/extraction reactions of lithium ions, leading to the improvement of the reaction kinetics. 5% Li_3PO_4-coated $LiNi_{0.5}Mn_{1.5}O_4$ exhibits the lowest charge-transfer resistance and the highest lithium diffusion coefficient among all samples, and it thus shows higher discharge capacities and better rate capability than the pristine material. The improved electrochemical properties also can be attributed that the Li_3PO_4 coating layer retards the side reactions of the active material with electrolyte. Hence, it is reasonable to infer that the Li_3PO_4 coating would be an effective way to improve the electrochemical properties of $LiNi_{0.5}Mn_{1.5}O_4$ cathode materials.

References:

[1] LIU Dong-Qiang(刘东强),YU Ji(吁霁), SUN Yu-Heng(孙玉恒), et al. *Chinese J. Inorg. Chem.*(无机化学学报), **2007**,**23**(1):41-45

[2] CHEN Zhao-Yong(陈召勇), LIU Xing-Quan(刘兴泉), GAO Li-Zhen(高利珍), et al. *Chinese J. Inorg. Chem.*(无机化学学报), **2001**,**17**(3):325-330

[3] WANG Chao(王超), LIU Xing-Quan(刘兴泉), LIU Hong-Ji(刘宏基), et al. *Chinese J. Inorg. Chem.*(无机化学学报), **2012**,**28**(9):1835-1842

[4] LIU Xing-Quan(刘兴泉), ZHONG Hui(钟辉), TANG Yi(唐毅), et al. *Chinese J. Inorg. Chem.*(无机化学学报), **2003**,**19**(5):467-472

[5] Yi T F, Yin L C, Ma Y Q, et al. *Ceram. Int.*, **2013**,**39**(4):4673-4678

[6] NIE Xiang(聂翔), Guo Xiao-Dong(郭孝东), ZHONG Ben-He(钟本和), et al. *Chinese J. Inorg. Chem.*(无机化学学报), **2012**,**28**(12):2573-2580

[7] Zhong Q, Bonakdarpour A, Zhong M, et al. *J. Electrochem. Soc.*, **1997**,**144**(1):205-213

[8] Wang J, Lin W, Wu B, et al. *J. Mater. Chem. A*, **2014**,**2**(48):16434-16442

[9] ZHANG Sheng-Li(张胜利), LI Liang-YU(李良玉), SONG Yan-Hua(宋延华), et al. *Rare Metal Mater. Eng.*(稀有金属材料与工程), **2010**,**39**(3): 515-518

[10]DENG Hai-Fu(邓海福), NIE Ping(聂平), SHEN Lai-Fa(申来法), et al. *Prog. Chem.*(化学进展), **2014**,**26**(6):939-949

[11]Wang S, Li P, Shao L, et al. *Ceram. Int.*, **2015**,**41**(1):1347-1353

[12]Li H, Luo Y, Xie J, et al. *J. Alloys Compd.*, **2015**,**639**:346-351

[13]WANG Zhao-Xiang(王兆翔), CHEN Li-Quan(陈立泉), HUANG Xue-Jie(黄学杰). *Prog. Chem.*(化学进展), **2011**,**23**(2/3):284-301

[14]Konishi H, Suzuki K, Taminato S, et al. *J. Power Sources*, **2014**,**269**:293-298

[15]Li X, Guo W, Liu Y, et al. *Electrochim. Acta*, **2014**,**116**:278-283

[16]Arrebola J C, Caballero A, Hernán L, et al. *J. Power Sources*,

2010,**195**(13):4278-4284

[17]Kim J W, Kim D H, Oh D Y, et al. *J. Power Sources*, **2015**, **274**:1254-1262

[18]Elia G A, Nobili F, Tossici R, et al. *J. Power Sources*, **2015**, **275**:227-233

[19]Zhang X, Cheng F, Yang J, et al. *Nano Lett.*, **2013**,**13**(6): 2822-2825

[20]Zhu Z, Zhang D, Yan H, et al. *J. Mater. Chem. A*, **2013**,**1** (18):5492-5496

[21]Zhu Z, Yan H, Zhang D, et al. *J. Power Sources*, **2013**,**224**: 13-19

[22]Liu G, Kong X, Sun H, et al. *Ceram. Int.*, **2014**,**40**(9):14391 -14395

[23]Myung S T, Komaba S, Kumagai N, et al. *Electrochim. Acta*, **2002**,**47**(15):2543-2549

[24]Wen L, Lu Q, Xu G. *Electrochim. Acta*, **2006**,**51**(21):4388-4392

[25]Xue Y, Wang Z, Yu F, et al. *J. Mater. Chem. A*, **2014**,**2**(12): 4185-4191

[26]Feng J, Huang Z, Guo C, et al. *Appl. Mater. Interfaces*, **2013**,**5**(20):10227-10232

[27]Yi T F, Fang Z K, Xie Y, et al. *Electrochim. Acta*, **2014**, **147**:250-256

[28]Zhang S Q, Xie S, Chen C H. *Mater. Sci. Eng. B*, **2005**,**121** (1/2):160-165

[29]Li X, Yang R, Cheng B, et al. *Mater. Lett.*, **2012**,**66**(1):168-171

[30]Jin N L Y, Chen C H, Wei S Q. *Electrochem. Solid-State Lett.*, **2006**,**9**(6):A273-A276

[31]Zhao S X, Ding H, Wang Y C, et al. *J. Alloys Compd.*, **2013**,**566**:206-211

[32]Wang L, Li H, Huang X, et al. *Solid State Ionics*, **2011**,**193** (1):32-38

[33]Yi T F, Zhu Y R, Zhu R S. *Solid State Ionics*, **2008**,**179** (38):2132-2136

[34]Kim J H, Yoon C S, Myung S T, et al. *Electrochem. Solid-State Lett.*, **2004**,**7**(7):A216-A220

[35]Kunduraci M, Amatucci G G. *J. Electrochem. Soc.*, **2006**, **153**(7):A1345-A1352

[36]Kunduraci M, Al-Sharab J F, Amatucci G G. *Chem. Mater.*, **2006**,**18**(15):3585-3592

[37]Aurbach D. *J. Power Sources*, **2000**,**89**(2):206-218

[38]Yang L, Takahashi M, Wang B. *Electrochim. Acta*, **2006**,**51** (16):3228-3234

[39]Gao X W, Deng Y F, Wexler D, et al. *J. Mater. Chem. A*, **2015**,**3**(1):404-41

[40]Yi T F, Chen B, Zhu Y R, et al. *J. Power Sources*, **2014**, **247**:778-785

[41]Yi T F, Xie Y, Wu Q, et al. *J. Power Sources*, **2012**,**214**: 220-226

[42]Hjelm A K, Lindbergh G. *Electrochim. Acta*, **2002**,**47**(11): 1747-1759

[43]Liu H, Wen G, Bi S, et al. *Electrochim. Acta*, **2015**,**171**: 114-120

[44]Yi T F, Yang S Y, Zhu Y R, et al. *Int. J. Hydrogen Energy*, **2015**,**40**(27):8571-8578

[45]SU Jing(苏婧), WU Xing-Long(吴兴隆), GUO Yu-Guo(郭玉国). *J. Inorg. Mater.*(无机材料学报), **2013**,**28**(11):1248-1254

[46]Yi T F, Li C Y, Zhu Y R, et al. *Russ. J. Electrochem.*, **2010**,**46**(2):227-232

[47]Beaulieu L Y, Larcher D, Dunlap R A, et al. *J. Electrochem. Soc.*, **2000**,**147**(9):3206-3212

[48]Bian X, Fu Q, Bie X, et al. *Electrochim. Acta*, **2015**,**174**: 875-884